

1
2
3
4
5
6
7
8
9
10
11
12
13
14

Ozonesonde Quality Assurance: The JOSIE-SHADOZ (2017) Experience

Anne M. Thompson^{1*}, Herman G. J. Smit², Jacquelyn C Witte^{1,3}, Ryan M. Stauffer^{1,4}, Bryan J. Johnson⁵, Gary Morris⁶, Peter von der Gathen⁷, Roeland Van Malderen⁸, Jonathan Davies⁹, Ankie Piters¹⁰, Marc Allaart¹⁰, Françoise Posny¹¹, Rigel Kivi¹², Patrick Cullis^{5,13}, Nguyen Thi Hoang Anh¹⁴, Ernesto Corrales¹⁵, Tshidi Machinini¹⁶, Francisco R. da Silva¹⁷, George Paiman¹⁸, Kennedy Thiong'o¹⁹, Zamuna Zainal²⁰, George B. Brothers^{21,22}, Katherine R. Wolff^{3,22}, Tatsumi Nakano²³, Rene Stübi²⁴, Gonzague Romanens²⁴, Gert J. R. Coetzee¹⁶, Jorge A. Diaz¹⁵, Sukarni Mitro¹⁸, Maznorizan 'bt Mohamad²⁰, Shin-Ya Ogino²⁵

15 12 August 2018

17 ¹ NASA Goddard Space Flight Center, Greenbelt, MD

18 ² Institute of Chemistry and Dynamics of the Geosphere: Troposphere, Research Centre Jülich,
19 Jülich, Germany

20 ³ Science Systems and Applications Inc., Lanham, MD

21 ⁴ Universities Space Research Association, Columbia, MD

22 ⁵ NOAA Earth System Research Laboratory, Global Monitoring Division, Boulder, CO

23 ⁶ St. Edwards University, Natural Sciences, Austin, TX

24 ⁷ Alfred Wegener Institute, Potsdam, Germany

25 ⁸ Royal Meteorological Institute of Belgium, Brussels, Belgium

26 ⁹ Environment and Climate Change Canada, Toronto, Ontario, Canada

27 ¹⁰ Royal Dutch Meteorological Institute, de Bilt, The Netherlands

28 ¹¹ Laboratoire de l'Atmosphère et des Cyclones, UMR8105 (Université, Météo- France, CNRS), La
29 Réunion, France

30 ¹² Finnish Meteorological Institute, Sodankylä, Finland

31 ¹³ Cooperative Institute for Research in Environmental Sciences, Boulder, CO

32 ¹⁴ Vietnam Meteorological Hydrological Administration, Ha Noi, Vietnam

33 ¹⁵ University of Costa Rica, San José, San Pedro, Costa Rica

34 ¹⁶ South African Weather Service, Pretoria, South Africa

35 ¹⁷ Laboratory of Environmental and Tropical Variables, Brazilian Institute of Space Research, Natal,
36 Brazil

37 ¹⁸ Meteorological Service of Suriname, Paramaribo, Surinam

38 ¹⁹ Kenyan Meteorological Department, Nairobi, Kenya

39 ²⁰ Malaysian Meteorological Department, Atmospheric Science and Cloud Seeding Division,
40 Petaling Jaya, Selangor, Malaysia

41 ²¹ CHEMAL, Wallops Is., VA

42 ²² NASA Wallops Flight Facility, Wallops Is., VA

43 ²³ Japan Meteorological Agency, Tokyo, Japan

44 ²⁴ MeteoSwiss, Payerne, Switzerland

45 ²⁵ Japan Agency for Marine-Earth Science and Technology, Department of Coupled Ocean-
46 Atmosphere-Land Processes Research, Yokosuka, Japan

47

48 *Corresponding Author: anne.m.thompson@nasa.gov; 301-614-5905; NASA/GSFC

49

50

51
52 Abstract. The ozonesonde is a small balloon-borne instrument that is attached to a standard
53 radiosonde to measure profiles of ozone from the surface to 35 km with ~100-m vertical
54 resolution. Ozonesonde data constitute a mainstay of satellite calibration and are used for
55 climatologies and analysis of trends, especially in the lower stratosphere where satellites are
56 most uncertain. The electrochemical-concentration cell (ECC) ozonesonde has been deployed at
57 ~100 stations worldwide since the 1960s, with changes over time in manufacture and procedures,
58 including details of the cell chemical solution and data processing. As a consequence, there are
59 biases among different stations and discontinuities in profile time-series from individual site
60 records. For 22 years the Jülich [Germany] Ozone Sonde Intercomparison Experiment (JOSIE)
61 has periodically tested ozonesondes in a simulation chamber designated the World Calibration
62 Centre for Ozonesondes (WCCOS) by WMO. In October-November 2017 a JOSIE campaign
63 evaluated the sondes and procedures used in SHADOZ (Southern Hemisphere Additional
64 Ozonesondes), a 14-station sonde network operating in the tropics and subtropics. A distinctive
65 feature of the 2017 JOSIE was that the tests were conducted by operators from eight SHADOZ
66 stations. Experimental protocols for the SHADOZ sonde configurations, which represent most
67 of those in use today, are described, along with preliminary results. SHADOZ stations that
68 follow WMO-recommended protocols record total ozone within 3% of the JOSIE reference
69 instrument. These results and prior JOSIEs demonstrate that regular testing is essential to
70 maintain best practices in ozonesonde operations and to ensure high-quality data for the satellite
71 and ozone assessment communities.

72 **Capsule:** Data from ozonesondes form a backbone of satellite algorithms and monitoring
73 stratospheric ozone recovery. The ozonesonde community regularly evaluates sonde procedures
74 and instrumentation, as in this experiment featuring operators from the tropical SHADOZ

75 network.

76

77 **JOSIE History and Background**

78 The periodic ozone assessments sponsored by WMO/UNEP (1991; 1995; 2011; 2015) and
79 related studies have long recognized the role of ozonesondes in the suite of global observations
80 because sondes are the only technique practical for in-situ monitoring of profiles. The sonde
81 instrument is easy to deploy in remote locations and is relatively inexpensive. Sondes operate in
82 both troposphere and stratosphere (Sidebar 1) and in clouds, precipitation and periods of
83 darkness. Most important, as they ascend, ozonesondes measure ozone with an effective
84 resolution of 100-150 m, far better than satellites. Indeed, sondes, like the ground-based
85 networks of lidar, Dobson and other spectrometers, constitute an essential component of satellite
86 calibration and cross-calibration (Fishman et al., 2008; Hubert et al., 2016; Steinbrecht et al.,
87 2017; Tarasick et al., 2018). The vertical structure of ozone as measured at a typical tropical
88 station appears in Sidebar 1, along with background on ozone in the atmosphere. Although
89 dozens of stations began launching ozonesondes in the 1970s and 1980s, the concepts of
90 standardizing and testing instruments in a coordinated network, did not evolve until the 1990s
91 (Mohnen, 1996; Melamed et al., 2015). This was the period when both the Jülich Ozone Sonde
92 Intercomparison Experiment (JOSIE) and Southern Hemisphere Additional Ozonesondes
93 (SHADOZ) project began.

94 **[Insert Sidebar 1 Here]**

95 Over 50 years of ozonesonde data-taking, there have been several instrument designs.
96 Furthermore, as instruments have changed and preparation and data-processing techniques have
97 evolved over time, time series of data from individual stations often display discontinuities and
98 gaps that lead to inhomogeneous data records. Thus, the reliability of ozonesonde trends was

99 questioned in some of the earlier ozone assessments (WMO/UNEP 1991; 1995;
100 SPARC/IOC/GAW, 1998) (See Acronym List).

101 Two approaches have been used to address these deficiencies. First, evaluations of
102 ozonesonde types in a controlled laboratory environment were undertaken in the 1990s, a process
103 that continues periodically to this day. Second, in a similar manner, by testing different sonde
104 preparation methods and protocols for data recording and processing, a set of standard operating
105 procedures (SOP; Smit et al., 2014) was developed through consensus with the ozonesonde
106 research community. Finally, there are recommended methods for reprocessing long-term
107 records compromised by inhomogeneities (Smit et al., 2012, Deshler et al., 2017).

108 The need to have recommended instruments and procedures for emerging WMO/GAW
109 stations in the 1990s provided a framework for the first intercalibration and intercomparisons of
110 existing ozonesonde types. In order to assess the performance of the various ozonesonde
111 instrument types used within GAW, the environmental simulation chamber (ESC) at the
112 Forschungszentrum Jülich (FZJ, Germany) was established as the World Calibration Centre for
113 Ozone Sondes (WCCOS) in 1996. The chamber enables control of pressure, temperature, and
114 ozone concentration as it simulates flight conditions of ozone soundings up to an altitude of 35
115 km (Smit et al., 2000). This controlled environment and comparison of the ozonesonde profiles
116 with an accurate UV-photometer as a reference (Proffitt and McLaughlin, 1983) are essential
117 requirements for addressing instrument issues that arise from field and laboratory operations.

118 The initial JOSIE, performed in 1996 (Smit and Kley, 1998), was the first GAW activity
119 directed toward implementing a global quality assurance plan for ozonesondes in routine use.
120 By now, JOSIE experiments have provided over twenty years of ozonesonde data quality
121 assurance to the larger atmospheric research and remote sensing communities. JOSIE-1996 was
122 attended by eight laboratories from seven countries representing the major types of ozonesondes:

123 Electrochemical Concentration Cell (ECC) sondes of two manufacturers, the Brewer/Mast sonde
124 (BM-original), the Indian sonde (a modified BM-type), and the Japanese Meisei sonde (KC79).
125 JOSIE-1996 revealed important information not only about ozonesonde performance but also the
126 influence of operating procedures for sonde preparation and data correction that often varied
127 among the participating laboratories. The succession of JOSIE campaigns (**Table 1**) has shown
128 that there is an on-going need to evaluate ozonesondes because the instruments, preparation
129 procedures, and/or the sensing solutions are modified, often inadvertently, over time. Routine
130 testing of newly manufactured ozonesondes on a regular basis coupled with better
131 standardization of operating procedures help ensure more confidence in the data itself as well as
132 trends calculated from the data.

133 The overall objective of WCCOS and the JOSIE series of experiments has been the
134 establishment of a facility for ozonesonde quality assurance (QA) that can be used by sonde
135 manufacturers and the research community. Instrumental performance of sondes from different
136 manufacturers is tested through comparison of profiling capabilities with a standard ozone
137 profile that simulates a typical ascent in polar, mid-latitude or tropical conditions. Regular
138 evaluation of procedures and methods at long-term ozone sounding stations with a single ozone
139 reference instrument ensures the traceability and consistency of the records.

140 Over time, the SOP have been established and updated as needed. The first major SOP
141 documentation appeared as a WMO/GAW Report (#201; See Smit and ASOPOS, 2014) with
142 major contributions from prior reports and Smit et al. (2007). GAW 201 was also based on field
143 tests of the major sonde types used in the JOSIEs up through 2009. A gondola of 18 instruments
144 was flown along with same UV-photometer used in JOSIE-2000 as reported in Deshler et al.
145 (2008).

146

147 **SHADOZ and Unresolved Sonde Issues**

148 The SHADOZ network began in 1998 as an international partnership to enhance the
149 number of tropical ozone soundings from operational stations (Thompson et al., 2003a,b; 2004;
150 2007; 2011). SHADOZ uses ECC ozonesondes that, over time, have been coupled with a variety
151 of radiosondes (**Table 2**). A history of ozonesonde-radiosonde pairings used at SHADOZ sites
152 appear in archival papers (Thompson et al., 2003a,b; Thompson et al., 2007; Witte et al., 2017).
153 At the time SHADOZ began, all known operational stations were in the southern hemisphere, but
154 gradually northern hemisphere stations joined: Kuala Lumpur, Paramaribo, Costa Rica; Hanoi,
155 and Hilo. The 14 long-term stations, defined as operating at least a decade during SHADOZ,
156 appear in **Fig. 1**. More than 7000 sets of ozone and pressure-temperature-humidity profiles from
157 SHADOZ are available at the website: <https://tropo.gsfc.nasa.gov/shadoz>.

158 Periodic evaluations of SHADOZ data have examined three parameters. First, total
159 column ozone (TCO) from the sonde, with an appropriate extrapolation above balloon burst, e.g.,
160 McPeters and Labow, (2012), is compared to TCO from co-located ground-based instruments
161 (Brewer, Dobson, SAOZ) and satellite overpasses. Second, stratospheric profiles are compared
162 to satellite overpass ozone profiles from instruments like SAGE II (to 2005), SBUV (entire
163 record, 1998-2016) or Aura's MLS (2005-). Third, for the tropical stations (generally within 18°
164 latitude of the equator), stratospheric column ozone and profiles are compared. The tropical
165 TCO is typically constant to within 3-5 DU (Dobson Units), so measurement biases from station
166 to station can be identified (Thompson et al., 2017).

167 The first three years of SHADOZ TCO compared to the EP/TOMS satellite TCO disagreed
168 by ~8% on average, with a number of stations displaying a discrepancy of greater than 10%; the
169 sonde TCO was usually lower than the satellite (or ground-based instrument). After the JOSIE-
170 2000 campaign (Smit et al., 2007), in which the instruments and techniques used at all the

171 SHADOZ stations were tested, several stations changed their sensing solution type (SST),
172 resulting in reduced offsets (Thompson et al., 2007). Further changes in sonde preparation
173 procedures and subsequent reprocessing of the data, both in accordance with WMO/SPARC/
174 IOC/NDACC guidelines (Smit and O3S-DQA, 2012; Smit and ASOPOS, 2014), brought TCO
175 for 12 of 14 stations to within 2% of TCO from three BUV-type satellites (EP/TOMS, OMI and
176 OMPS) operating over the 1998-2016 period (Thompson et al., 2017); the remaining two stations
177 show TCO data averaging within 5% of the satellite TCO. These improvements derive from the
178 application of “transfer functions” that relate a profile from each instrument–SST combination to
179 data from the standard reference. Each profile in a time-series is examined for possible
180 correction (Witte et al., 2017; 2018).

181 Although the reprocessing of prior SHADOZ data has greatly reduced systematic variations
182 in the record, JOSIE-SHADOZ was designed to address several outstanding issues. First, transfer
183 functions determined by Deshler et al. (2017) are used to homogenize SHADOZ readings that
184 are taken with different SST and/or instruments. This includes the 1%, KI, 0.1% buffer SST
185 used at stations supported by NOAA since the mid-2000s (Sterling et al., 2018). Second, a few
186 stations in SHADOZ changed SST unintentionally and introduced discontinuities in station time-
187 series (Thompson et al., 2017; Witte et al., 2017; 2018). Finally, several stations employing a
188 given sonde type show sharp discontinuities after 2014 that appear to originate with changes in
189 manufacture (Sterling et al., 2018; Thompson et al., 2017).

190 **[Insert Sidebar 2 here]**

191

192 **JOSIE-SHADOZ-2017 Goals**

193 Similar to prior JOSIE campaigns, the major objectives of JOSIE-SHADOZ are:

194 1. Evaluate ozonesonde instrument performance, specifically the pump and sensor as delivered

195 by the ECC-sonde manufacturer. Most of the SHADOZ stations operate with WMO-
196 recommended solutions and preparation and calibration procedures that allow the
197 experimenters to update typical performance of the instruments relative to the Ozone
198 Photometer (OPM) reference instrument (Proffitt and McLaughlin, 1983).

- 199 2. Evaluate current preparation and operating procedures of each SHADOZ station. Unlike
200 prior JOSIE experiments, in 2017 personnel representing the practices of all currently
201 operating SHADOZ stations participated (**Tables 2 and 3; see Sidebar 2**). In most cases the
202 operators supplied solutions as prepared at their home institution. In the first part of the
203 JOSIE-2017, the operators followed their standard practice for pre-conditioning sondes and
204 for “day of flight” prior to simulation in the ESC. The goal was to understand the existing
205 ozone profiles archived in SHADOZ by reproducing current practices, techniques, and
206 solutions at each participating station as closely as possible.
- 207 3. Evaluate the current WMO recommended SOP. Specific instrumental aspects examined in
208 these tests were details of pre-conditioning, background current, response time, pump flow
209 efficiency, and SST. In addition to two WMO-recommended SST, two alternatives, one of
210 which is employed at several SHADOZ stations, were included in the tests.

211

212 **The Ozonesonde Design**

213 The electrochemical concentration cell (ECC) ozonesonde uses a chemical reaction
214 measured inside a pair of cells that is displayed schematically in **Fig. 3a**. As the sonde rises in
215 the atmosphere (and during the laboratory calibration phase), air is pulled through the intake tube
216 (left in **Fig. 3a**) and pushed into the cathode cell by means of a small pump. The pump
217 maintains positive pressure as the air is sampled; the flow rate is measured during pre-flight
218 calibration. The second cell (anode) is filled with a saturated version of the cathode solution and

219 is located adjacent to the cathode, with an ion bridge separating the two cells. The reacting
 220 chemical, oxidized by the ozone molecule, is dissolved potassium iodide (KI). The sensing
 221 solution is maintained at a neutral pH with the addition of the paired phosphates ($\text{NaH}_2\text{PO}_4 \cdot \text{H}_2\text{O}$ /
 222 $\text{Na}_2\text{HPO}_4 \cdot 12\text{H}_2\text{O}$). The ozone partial pressure is calculated by the following equation (taken
 223 from Witte et al. 2018),

$$224 \quad R_{\text{O}_3} = 4.307 \cdot 10^{-2} \frac{(I_{\text{M}} - I_{\text{B}}) T_{\text{R}}}{Y_{\text{R}} F_{\text{R}} h_{\text{C}}}$$

225 where

226 P_{O_3} = Ozone partial pressure, mPa

227 I_{M} = Cell current, μA

228 I_{B} = Cell background current, μA

229 T_{P} = Ozonesonde pump temperature, K

230 Φ_{P} = Pump flow-rate, ml/s

231 Ψ_{P} = Pump flow efficiency, unitless

232 η_{C} = Conversion efficiency which is generally assumed to be 1.

233

234 The pump flow efficiencies, Ψ_{P} , take into account the buffering of the solution, depending on the
 235 solution recipe, and mechanical degradation of the pump at low pressures (< 100 hPa). The
 236 volume mixing ratio is computed from the ratio of the ozone partial pressure (P_{O_3}) to the ambient
 237 pressure determined from the radiosonde attached to the ozonesonde container as the two
 238 instruments ascend into the stratosphere (**Fig. 3b**). The typical ascent rate is 5 m/s.

239 From the large body of SHADOZ data as well as instruments in the field and prior lab
 240 intercomparisons it is known that the two major sources of systematic error are the manufacture
 241 of the instrument and the composition of the KI and/or buffers in the SST (Smit et al., 2007).

242 Random sources of error include operator handling and changing conditions in the station
243 calibration unit. Calibration practices and the method of data-processing can also lead to
244 systematic differences among station profiles (Johnson et al., 2002; Deshler et al., 2008; 2017).
245 In JOSIE-SHADOZ two types of protocols investigated these issues. The first five of ten tests in
246 each session were carried out with the operators using their own solutions and preparation
247 technique. We refer to this as SHADOZ SOP (Standard Operating Procedure). In the second set
248 of tests, uniform calibration and preparation procedures were followed using JOSIE-prepared
249 solutions, hereafter referred to as the JOSIE SOP. Unified data collection by the Data
250 Acquisition System (DAS) eliminates variations due to operator data-processing.

251

252 *General Operations during JOSIE-SHADOZ (2017)*. The JOSIE-SHADOZ 2017 campaign
253 took place at the World Calibration Centre for Ozone Sondes (WCCOS) at the Research Center
254 Jülich (FZJ) in the Institute of Energy and Climate Research: Troposphere (IEK-8), Jülich,
255 Germany. Ozonesonde pre-conditioning test units and the ECC instruments were provided by
256 FZJ from a pool of loaned supplies. Participants were split into two groups (**Table 3**), each of
257 four teams operating ozonesondes of the type used in SHADOZ (**Table 2**). Each group
258 participated in a 12-day intercomparison campaign. Session No. 1 took place from 9 to 20
259 October 2017; Session No. 2 took place from 23 October through 3 November 2017. Each
260 session consisted of ten simulation experiments with all four participant sondes being “flown”
261 simultaneously in the chamber (see **Sidebar 3**) to an effective altitude of ~35 km. The overall
262 protocol for each campaign was similar but the second session tested two “JOSIE SSTs” (**Table**
263 **4**). During the SHADOZ SOP (first five simulations) participants used their own zero-air filter,
264 solutions, and preparation procedures. During the JOSIE SOPs the lab provided a single source

265 of high-quality zero-air, a common SST, and common operating procedures that all teams
 266 followed. Data were collected by the DAS of the WCCOS test chamber.

267 **[Insert Sidebar 3 here]**

268 Because JOSIE-SHADOZ 2017 was focused on questions about SHADOZ operations, all
 269 the chamber runs simulated tropical sounding conditions (**Fig. 4**). The test profiles described in
 270 **Fig. 4** and **Table 4** represent three typical tropical profiles, one that is unpolluted throughout the
 271 troposphere with very low ozone near the tropopause and two with higher levels of ozone in the
 272 free troposphere and near the tropopause.

273 Four SST recipes were tested. All sonde data were processed by using a constant
 274 background current correction. Total ozone column normalization was not applied. The
 275 solutions, with references, follow:

276 1. SHADOZ 1.0. The WMO-recommended SOP (Smit et al., 2012) for use with the
 277 Science Pump (SPC) instrument and is referred to as SST 1.0%-Full Buffer:

278 Cathode: 1% KI + Full-Buffer & KBr as described by Komhyr (1986)

279 Anode: Cathode solution with saturated KI

280 Pump flow efficiency factors (PEF): Komhyr (1986)

281 2. SHADOZ 0.5. The WMO-recommended SOP (Smit et al., 2012) for use with the ENSCI
 282 instrument is referred to as SST 0.5%-Half Buffer:

283 Cathode: 0.5% KI + Half of the Buffer & KBr as described by Komhyr et al. (1995)

284 Anode: Cathode solution with saturated KI

285 PEF: Komhyr et al. (1995)

286 3. JOSIE 1.0.1. Solution developed by NOAA for use with ENSCI sondes that has been
 287 employed at Fiji, Samoa, Costa Rica, and Hilo stations since the late 2000's. The
 288 formulation is SST 1.0%-1/10th Buffer:

289 Cathode: 1% KI+ 1/10th Buffer, KBr as described by Komhyr (1986)
290 Anode: Cathode solution with saturated KI
291 PEF: New constants derived from recent pumpflow measurements made by
292 Nakano (2017, private communication).

293 4. JOSIE 2.0.1. This variation on JOSIE 1.0.1 was used to test if ozone response in the
294 tropopause and stratosphere regions is improved by doubling the KI concentration:

295 Cathode: 2% KI + 1/10th Buffer, KBr as described by Komhyr (1986)
296 Anode: Cathode solution with saturated KI
297 PEF: New constants derived from recent pumpflow measurements made by
298 Nakano (2017, private communication).

299

300 **Preliminary Results**

301 Preliminary data are used to answer three questions. (1) What is the accuracy of ozone
302 readings throughout the profile for each sonde-SST combination tested in the ESC? This is
303 answered by comparing both the ozone partial pressure profiles measured by the sonde with the
304 OPM and column-integrated ozone from the sondes with the OPM. For the latter, TCO and
305 segments for troposphere, stratosphere and the tropopause transition layer (TTL) in between the
306 stratosphere and troposphere are computed. (2) How do profiles and column segments from
307 sondes prepared with the SHADOZ SOP compare to those prepared with the JOSIE SOP? (3)
308 What differences are observed when the same instrument type is prepared with different SST or
309 when different instruments use the same SST? Differences are expected based on prior JOSIE
310 results and field tests.

311 **SHADOZ SOP.** Fig. 5 displays raw data from eight SHADOZ participants. The OPM

312 measurements are represented by the black dashed lines: **Fig. 5a** shows the data for a simulation
313 in Session 1 (No. 171) and **Fig. 5b** for a simulation in Session 2 (No. 182). The fundamental unit
314 in the tests is lapsed time; quoted “altitudes” are approximate. There is some arbitrariness in
315 designating the TTL, with lower-mid-troposphere below and mid to upper stratosphere above.
316 We adopt a TTL at 2200-3800 s (~12-18 km) when analyzing the test results. In this region the
317 signal-to-noise ratio is low, and therefore the uncertainty, is highest (Witte et al., 2017).

318 In **Fig. 5a** the ozone partial pressures are very small throughout the “troposphere” and up
319 to ~3500 s or ~17.5 km. This profile simulates a near-zero-ozone tropopause, mimicking
320 western Pacific profiles (Kley et al., 1996; Thompson et al., 2012; Rex et al., 2014; Newton et
321 al., 2016), where SNR in ozone readings is often low. In **Fig. 5b** ozone partial pressure
322 throughout the tropospheric profile is higher, representing stations influenced by biomass
323 burning pollution in the lower-mid troposphere (Thompson et al., 1996; Jensen et al., 2012). The
324 ozone transition near the tropopause and in the lower stratosphere in Simulation No. 182 (**Fig.**
325 **5b**) lacks the sharp gradient intentionally generated in **Fig. 5a**. The pattern in **Fig. 5b** resembles
326 that of SHADOZ stations that exhibit gradual ozone transitions in the TTL, e.g., Ascension,
327 Natal and Nairobi. Their upper tropospheric and TTL cross-sections and their contributions to
328 the zonal wave-one in tropical ozone are summarized in Thompson et al. (2003b; 2011; 2017).

329 The OPM TCO in **Fig. 5a** is 282 DU. The TCO from the four participants in Session 1
330 are all higher than the OPM by 3-26 DU (up to 9%). The OPM TCO in **Fig. 5b** is 334 DU. The
331 TCO from the four participants in Session 2 are all equal to or higher than the OPM, with the
332 largest offset 23 DU (7%) higher. Columns 2 and 3 in **Table 5** list the corresponding TCO
333 fractions for all 8 participants relative to the OPM.

334 The means of five simulations for all eight participants, expressed as absolute and
335 percentage differences from the OPM and based on their SHADOZ SOP are displayed in **Fig. 6**.

336 The shapes of the mean profiles are broadly similar with the sonde partial pressures (relative to
337 the OPM, **Fig. 6a**) overlapping throughout the troposphere and TTL (to 3500s). In the
338 stratosphere (above 4000 s, ~20 km) differences are much larger. The fractional differences are
339 smaller in the stratosphere (**Fig. 6b**), however, because the ozone partial pressure peaks at over
340 20 mPa (**Fig. 5**). The relative differences with the OPM are largely within $\pm 10\%$ of the OPM
341 (zero-line in **Fig. 6b**) throughout the lower to mid-troposphere (0-2000 s, up to 10-12 km).
342 Around 2000 s, there is an inflection, with the offsets all turning more negative. The largest
343 relative differences occur within the upper troposphere (UT) and TTL (equivalent to 2500-3500
344 s, 13-18 km), exceeding 5% on average for all the stations. For participant nos. 4 and 5 the mean
345 relative differences exceed -20%. Witte et al. (2018) noted that SHADOZ ozone values are most
346 uncertain in the narrow region between 15 and 17 km (~3000-4300 s). However, the large
347 offsets recorded in **Fig. 6b** originate from four JOSIE tests conducted with TTL ozone equivalent
348 to 2 DU (e.g. Simulation 171, **Fig. 5a**); a value that applies to only ~ 5% of tropical SHADOZ
349 readings. Realistically, Fig. 8b in Thompson et al. (2017), based on > 6000 profiles, shows that
350 the actual TTL ozone for 12 of 14 SHADOZ stations is 8.0 ± 1.5 DU. By 3000 s (~15 km) the
351 relative differences of all SHADOZ profiles with respect to the OPM start to increase. All
352 SHADOZ profiles show excellent agreement with OPM to within $\pm 5\%$ at 20-25 km (critical
353 ozone maximum). By 5000 s (~ 25 km) most SHADOZ profiles exceed OPM ozone and are
354 well-aligned with one another. The range of mean deviations in the region corresponding to 20-
355 28 km is within 10%. This tighter clustering implies good measurement precision. By ~5500 s
356 (27.5 km) all the SHADOZ readings are higher than the OPM. Above 30 km the agreement
357 breaks down and there is a downturn in ozone readings relative to the OPM for most stations.
358 Exceptions are participant No. 1 and 7 that display +10% and 4% deviations, respectively (**Fig.**
359 **6b**). The negative relative differences are not surprising. Witte et al. (2017) showed that even

360 reprocessed SHADOZ ozonesonde data above ~30 km are highly variable and not as reliable.

361 How do column amounts for the SHADOZ participants compare on average to OPM
362 ozone? Answers appear in **Table 5**. For the five SHADOZ simulations all of the participants
363 record, on average, slightly more ozone than the OPM, with ratios from 1.017-1.040 (1.7% to
364 4.0% more O₃). This result seems to validate the quality assurance practices of the SHADOZ
365 stations, with 7 of 8 participants following the WMO-recommended instrument SST
366 combinations and SOP (Smit et al., 2007; 2012). The segment column comparisons (columns 0-
367 15 km, 12-18 km, 15 km-end in **Table 5**) demonstrate that the good agreement between sondes
368 and the OPM is dominated by the ozone column from 15 km-end, i.e., the stratospheric portion
369 of the profile. Because the WMO recommendations are largely based on JOSIE-2000, several
370 follow-on lab tests and the BESOS conducted in 2004, it can be inferred that the WMO
371 recommendations (Smit et al., 2012) are still valid. Agreement in the TTL (12-18 km column)
372 averages < 0.95 for half of the groups (**Table 5**). Because the OPM recorded only 5 DU on
373 average in this region, the larger offsets do not detract from the good agreement overall.

374 **JOSIE SOP.** The sonde partial pressure offsets from the OPM and relative differences
375 for the eight participants using the JOSIE 1.0.1 SST and preparation protocols appear in **Fig. 7a**
376 and **Fig. 7b**, respectively. When these results are compared to those with the SHADOZ SOP
377 (**Fig. 6**) two differences are observed. First, the divergence among stations is less with the more
378 uniform specifications of the JOSIE SOP, especially in the mid-troposphere through the TTL.
379 This is not surprising because the use of a single SST and SOP is expected to minimize
380 variations due to SST. The JOSIE SOP uses solutions with less buffer by a factor of 2 or 10.
381 Thus, due to the lower buffer the sonde responses show less hysteresis effect in the region with
382 relatively fast ozone changes, resulting in increased SNR. This is particularly true in the TTL at
383 the tropopause and just above, corresponding to the 2500 to 3500 s region in **Fig. 6b** and **Fig. 7b**.

384 The second difference is that ozone readings throughout the profile are lower relative to the
385 OPM with the JOSIE SOP than the SHADOZ SOP, particularly in the troposphere (**Fig. 7a**
386 below 4000 s) and even more so in the stratosphere, where the offsets are -1 to -2 mPa ozone.
387 The result is a mean sonde TCO offset with the JOSIE SOP relative to the OPM of 0.97 (first
388 two entries in column three of **Table 6**) compared to a mean 1.03 TCO offset with the SHADOZ
389 SOP. Background cell currents and response times improved significantly during the JOSIE SOP
390 in both sessions when a shared zero-air system was used.

391 *SHADOZ-JOSIE Comparisons.* **Fig. 8a** displays the average differences between the
392 SHADOZ and JOSIE SOP profiles for Session 1. For each participant in Session 1, five
393 simulations were made totaling 20 profiles of each SOP, both using the same SST. Up to 10 km
394 the SHADOZ SOP resulted in relatively higher ozone readings; toward the TTL the JOSIE SOP
395 resulted in higher ozone readings. The stratospheric differences, however, show the JOSIE SOP
396 averages 3% lower TCO than the OPM while the SHADOZ SOP averages 3% higher TCO than
397 the OPM (and stratospheric segment, **Table 6**). Note that the near-zero simulated ozone
398 represents a small fraction of what is observed in SHADOZ records; thus, the large uncertainties
399 seen in **Fig. 8a** represent the extrema of the data set.

400 In Session 2, to compensate for the reduced sensitivity of the 1.0%, 1/10th Buffer SST
401 (JOSIE 1.0.1), solutions with the JOSIE SOP were prepared with twice as much KI but the same
402 low buffer, the so-called JOSIE 2.0.1. JOSIE 1.0.1 comparisons were all made with ENSCI,
403 whereas the JOSIE 2.0.1 referred to a combination of SPC and ENSCI. Mean profile
404 comparisons with the different SSTs are summarized in **Fig. 8b**. The differences are not
405 statistically significant throughout the troposphere or TTL but the JOSIE 2.0.1 profile mean is
406 closer to the OPM in the upper stratosphere (above 5000 s). In Session 2, the ratio of sonde to
407 OPM partial column ozone above 20 km for JOSIE 1.0.1 was 0.95, while for JOSIE 2.0.1 it was

408 0.97. Sondes filled with both SST show sondes measure less ozone than the OPM in the
409 stratosphere and are highly variable above 30 km, consistent with **Fig. 7** and Witte et al. (2018)
410 findings.

411 Previous JOSIE campaigns and various field tests (especially the BESOS in 2004) noted that
412 throughout the ozone profile when the same SST is used, the ENSCI instrument tends to measure
413 more ozone than the SPC instrument. Of the 14 SHADOZ stations, 11 use the ENSCI
414 instrument and three use the SPC type (Thompson et al., 2017; Witte et al., 2017; 2018). **Fig. 8c**,
415 based on the combined session simulations (JOSIE 1.0.1), shows that, also for the less buffered
416 solutions, the ENSCI instrument measures slightly higher ozone than the SPC with the greatest
417 discrepancies in the troposphere, consistent with previous JOSIE studies.

418

419 **Conclusions**

- 420 1. All 8 stations participating in JOSIE-SHADOZ-2017 measured ozone that agreed well
421 with the OPM.
- 422 2. The slight ENSCI – SPC ozone bias (ENSCI reads higher) previously observed (Smit et
423 al., 2007; 2012) remained in JOSIE-SHADOZ 2017.
- 424 3. JOSIE-2017 affirms the very high quality of the SHADOZ methods that use SOP and
425 SST-instrument combinations based on earlier JOSIE campaigns and field tests as
426 summarized in Smit et al. (2007; 2012). This is independent confirmation of the
427 accuracy of the large SHADOZ dataset that up to now has only been compared to data
428 from satellite and ground-based instruments (Thompson et al., 2017; Witte et al., 2017).
429 The ozonesonde community goals of “5% accuracy and precision in TCO” has been met
430 by SHADOZ operators engaging in collaborative ozonesonde “expert” activities since
431 2000. Except for the TTL, most instrument-SST combinations tested in JOSIE with

432 SHADOZ SOP agreed within 3% of OPM in total column amount (sonde higher) and 5-
433 10% throughout the ozone profile. The often large TTL ozone underestimate (>30%
434 relative to OPM in some tests) contributes only 2-3% of the total ozone column.

435 4. JOSIE tested solutions with a reduced buffer SST, of the type used at four SHADOZ
436 stations. As expected, agreement of sonde ozone data with the OPM in the TTL regions
437 was improved. However, sensitivity to stratospheric ozone is reduced, so TCO from
438 these tests averaged 3% lower than the OPM. The low-bias is reduced when the KI is
439 doubled (JOSIE2.0.1). However, the divergence of profiles with the different SST is so
440 small (~5%) that further analysis, such as taking into account individual sonde responses,
441 is required.

442 5. JOSIE SOP:

- 443 • Lower, uniform, and better reproducible background cell currents are achieved
444 using a high quality no-ozone filter source or purified air.
- 445 • The hysteresis effect ('memory' effect due to the buffering of the solution) is
446 minimized which may improve the response of the sonde, particularly in the TTL
447 where sharp ozone gradients are measured.

448
449 Because SHADOZ represents virtually all current ECC sonde practices used by the
450 global ozone community, these findings and any SOP recommendations that ozonesonde
451 "experts" consider in light of JOSIE-2017 should be universally valid for ECC instruments.
452 Establishing SOP guidelines and standardization of ground equipment is essential to achieving
453 an uncertainty less than 5% between surface and 30 km altitude. The JOSIE-SHADOZ 2017
454 experience highlights the necessity of having a continuous reference calibration facility
455 (WCCOS) operating over the past 25 years. The capacity building exercise has empowered

456 participants to continue working towards ensuring high quality standard in sonde data-taking.
457 With well-trained and motivated operators, SOPs based on best practices, and experiments such
458 as JOSIE-SHADOZ, our aim of an uncertainty less than 5% can be achieved.

459

460 **Acknowledgments.** The 2017 JOSIE would not have been possible without strong support of
461 the IEK-8 group of Forschungszentrum-Jülich including a number of technicians and Ms. Gabi
462 Nork who was in charge of the organizing. The United Nations Environmental Programme (S.
463 Mylona, Nairobi) provided travel funds for SHADOZ operators. Support was also given by the
464 Science Pump Corporation (S. Schwartz), ENSCI (J. Harnetiaux and G. Kok) and JAMSTEC (S-Y.
465 Ogino). SHADOZ is supported by NASA's Upper Atmosphere Research Program and Aura
466 Validation, NOAA's Global Monitoring Division Lab (Boulder) and more than 15 organizations in
467 SHADOZ host nations and from Japan, Switzerland, France and the Netherlands.

468

469 **ACRONYMS**

470 ASOPOS = Assessment of SOP for Ozone Sondes

471 DAS = Data Acquisition System

472 ECC = Electrochemical Concentration Cell

473 ENSCI = Environmental Science Corp.

474 ESC = Environmental Simulation Chamber

475 FZJ = Forschungszentrum - Jülich

476 GAW = Global Atmospheric Watch

477 GSFC = Goddard Space Flight Center

478 IOC = International Ozonesonde Commission

479 JAMSTEC = Japan Agency for Marine-Earth Science and Technology

480 JOSIE = Jülich Ozonesonde Intercomparison Experiment

- 481 KNMI = Koninklijk Nederlands Meteorologisch Instituut
- 482 MLS = Microwave Limb Sounder
- 483 NDACC = Network for the Detection of Atmospheric Composition Change
- 484 OPM = Ozone Photometer
- 485 OPS = Ozone Profile Simulator
- 486 PEF = Pump Efficiency Factor
- 487 QA = Quality Assurance
- 488 SBUV = Solar Backscatter Ultraviolet
- 489 SHADOZ = Southern Hemisphere Additional Ozonesondes
- 490 SNR = Signal Noise Ratio
- 491 SOP = Standard Operating Procedures
- 492 SPARC = Stratospheric Processes And their Role in Climate
- 493 SPC = Science Pump Corporation
- 494 SST = Sensing Solution Type
- 495 TCO = Total Column Ozone
- 496 TTL= Tropical Tropopause Layer (or Tropopause Transition Layer)
- 497 UNEP = United Nations Environmental Programme
- 498 WMO = World Meteorological Organization
- 499 WCCOS = World Calibration Centre for Ozonesondes

500

501 **REFERENCES**

- 502 Deshler, T., J. Mercer, H. G. J. Smit, R. Stubi, G. Levrat, B. J. Johnson, S. J. Oltmans, R. Kivi, J.
- 503 Davies, A. M. Thompson, J. Witte, F. J. Schmidlin, G. Brothers and T. Sasaki (2007),
- 504 Atmospheric comparison of electrochemical cell ozonesondes from different manufacturers,

505 and with different cathode solution strengths: The Balloon Experiment on Standards for
506 Ozonesondes, *J. Geophys. Res.*, 113, D04307, doi: 10.1029/2007JD008975.

507 Deshler, T., R. Stübi, F. J. Schmidlin, J. L. Mercer, H. G. J. Smit, B. J. Johnson, R. Kivi and B.
508 Nardi (2017), Methods to homogenize electrochemical concentration cell (ECC) ozonesonde
509 measurements across changes in sensing solution concentration or ozonesonde manufacturer,
510 *Atmos. Meas. Tech.*, 10, 2021-2043, doi:10.5194/amt-10-2021-2017.

511 Fishman, J., K.W. Bowman, J. P. Burrows, A. Richter, K. V. Chance, D. P. Edwards, R. V.
512 Martin, G. A. Morris, R. B. Pierce, J. R. Ziemke, J. A. Al-Saadi, J. K. Creilson, T. K.
513 Schaack, and A.M. Thompson (2008), Remote sensing of tropospheric pollution from space,
514 *Bull. Amer. Meteor. Soc.*, 89, 805-821.

515 Hilsenrath, E., et al (1986), Results from the balloon ozone intercomparison campaign (BOIC),
516 *J. Geophys. Res.*, 91 (D12), 13137–13152, doi: 10.1029/JD091iD12p13137.

517 Hubert, D., et al., (2016), Ground-based assessment of the bias and long-term stability of 14 limb
518 and occultation ozone profile data records, *Atmos. Meas. Tech.*, 9, 2497-2534,
519 doi:10.5194/amt-9-2497-2016, 2016.

520 Jensen, A. A., A. M. Thompson, and F. J. Schmidlin (2012), Classification of Ascension Island
521 and Natal ozonesondes using self-organizing maps, *J. Geophys. Res.*, 117, D04302, doi:
522 10.1029/2011JD016573.

523 Johnson, B. J., S. J. Oltmans, H. Voemel, H. G. J. Smit, T. Deshler, and C. Kroeger (2002), ECC
524 Ozonesonde pump efficiency measurements and tests on the sensitivity to ozone of buffered
525 and unbuffered ECC sensor cathode solutions, *J. Geophys. Res.*, 107, D19 doi:
526 10.1029/2001JD000557.

- 527 Kley, D., P. J. Crutzen, H. G. J. Smit, H. Vömel, S. J. Oltmans, H. Grassl, and V. Ramanathan,
528 (1996). Observations of near-zero ozone concentrations over the convective Pacific: Effects
529 on air chemistry. *Science*, 274(5285), 230-233, doi: 10.1126/science.274.5285.230.
- 530 Komhyr, W.D. (1986), Operations handbook - Ozone measurements to 40 km altitude with
531 model 4A-ECC-ozone sondes, NOAA Techn. Memorandum ERL-ARL-149.
- 532 Komhyr, W. D., R. A. Barnes, G. B. Brothers, J. A. Lathrop and D. P. Opperman (1995),
533 Electrochemical concentration cell ozonesonde performance evaluation during STOIC 1989,
534 *J. Geophys. Res.*, 100(5) 9231-9244, doi:10.1029/94JD02175.
- 535 McPeters , R. D., and G. J. Labow (2012) Climatology 2011: An MLS and sonde derived ozone
536 climatology for satellite retrieval algorithms, *J. Geophys. Res.*, 117, D10303, doi:
537 10.1029/2011JD017006.
- 538 Melamed, M. L., P. S. Monks, A. H. Goldstein, M. G. Lawrence and J. Jennings (2016) The
539 international global atmospheric chemistry (IGAC) project: Facilitating atmospheric
540 chemistry research for 25 years, *Anthropocene*, [http://dx.doi.org/10.1016/](http://dx.doi.org/10.1016/j.ancene.2015.10.001)
541 [j.ancene.2015.10.001](http://dx.doi.org/10.1016/j.ancene.2015.10.001)
- 542 Mohnen, V. (1996), Update on IGAC's Global Tropospheric Ozone Network (GLONET)
543 Activity and the International Tropospheric Ozone Years (ITOY), IGACtivities, IGAC
544 Project Office, Boulder, CO, 4-6, ([http://igacproject.org/sites/default/files/2016-](http://igacproject.org/sites/default/files/2016-07/Issue_03_Jan_1996.pdf)
545 [07/Issue_03_Jan_1996.pdf](http://igacproject.org/sites/default/files/2016-07/Issue_03_Jan_1996.pdf))
- 546 Newton, R., G. Vaughan, H. M. A. Ricketts, L. L. Pan, A. J. Weinheimer and C. Chemel (2016),
547 Ozonesonde profiles from the West Pacific Warm Pool: measurements and validation,
548 *Atmos. Chem. Phys.*, 16, 619-634, doi:10.5194/acp-16-619-2016.

- 549 Proffitt, M.H., and R.J. McLaughlin (1983), Fast response dual-beam UV-absorption photometer
550 suitable for use on stratospheric balloons, *Rev. Sci. Instrum.*, 54, 1719-1728.
- 551 Rex, M., I. Wohltmann, T. Ridder, R. Lehmann, K. Rosenlof, P. Wennberg, D. Weisenstein, J.
552 Notholt, K. Krüger, V. Mohr and S. Tegtmeier (2014), A tropical West Pacific OH minimum
553 and implications for stratospheric composition, *Atmos. Chem. Phys.*, 14, 4827-4841,
554 <https://doi.org/10.5194/acp-14-4827-2014>.
- 555 Smit H. G. J and D. Kley (1998), JOSIE: The 1996 WMO International intercomparison of
556 ozonesondes under quasi flight conditions in the environmental simulation chamber at Jülich,
557 WMO Global Atmosphere Watch Report No. 130, WMO TD No. 926, World Meteorological
558 Organization, Geneva.
- 559 Smit H. G. J., W. Sträter, M. Helten and D. Kley (2000), Environmental simulation facility to
560 calibrate airborne ozone and humidity sensors. Jül Berichte Nr 3796, Forschungszentrum
561 Jülich, Germany.
- 562 Smit, H. G. J., W. Straeter, B. Johnson, S. Oltmans, J. Davies, D. W. Tarasick, B. Hoegger, R.
563 Stubi, F. Schmidlin, T. Northam, A. M. Thompson, J. Witte, I. Boyd and F. Posny (2007),
564 Assessment of the performance of ECC-ozonesondes under quasi-flight conditions in the
565 environmental simulation chamber: Insights from the Jülich Ozone Sonde Intercomparison
566 Experiment (JOSIE), *J. Geophys. Res.*, 112, D19306, doi:10.1029/2006JD007308.
- 567 Smit, H. G. J., and O3S-DQA (2012), Guidelines for homogenization of ozonesonde data,
568 SI2N/O3S-DQA activity as part of “Past changes in the vertical distribution of ozone
569 assessment”, available at: [http://www-](http://www-das.uwyo.edu/%7Edeshler/NDACC_O3Sondes/O3s_DQA/O3S-DQA-Guidelines%20Homogenization-V2-19November2012.pdf)
570 [das.uwyo.edu/%7Edeshler/NDACC_O3Sondes/O3s_DQA/O3S-DQA-](http://www-das.uwyo.edu/%7Edeshler/NDACC_O3Sondes/O3s_DQA/O3S-DQA-Guidelines%20Homogenization-V2-19November2012.pdf)
571 [Guidelines%20Homogenization-V2-19November2012.pdf](http://www-das.uwyo.edu/%7Edeshler/NDACC_O3Sondes/O3s_DQA/O3S-DQA-Guidelines%20Homogenization-V2-19November2012.pdf).

- 572 Smit, H. G. J., and the Panel for the Assessment of Standard Operating Procedures for
573 Ozonesondes (ASOPOS) (2014), Quality assurance and quality control for ozonesonde
574 measurements in GAW, World Meteorological Organization, GAW Report 201. [Available
575 at
576 http://www.wmo.int/pages/prog/arep/gaw/documents/FINAL_GAW_201_Oct_2014.pdf.]SP
577 ARC-IOC-GAW Assessment of Trends in the Vertical Distribution of Ozone (1998), SPARC
578 Report No.1, WMO Global Ozone Research and Monitoring Project Report No. 43, World
579 Meteorological Organization, Geneva.
- 580 Steinbrecht, W., et al. (2017) An update on ozone profile trends for the period 2000 to 2016,
581 *Atmos. Chem. Phys.*, 17, 10675-10690, <https://doi.org/10.5194/acp-17-10675-2017>.
- 582 Sterling, C. W., B. J. Johnson, S. J., Oltmans, H. J. G. Smit, A. F. Jordan, P. D. Cullis, E. G.
583 Hall, A. M. Thompson, and J. C. Witte (2018), Homogenizing and estimating the uncertainty
584 in NOAA's long-term vertical ozone profile records measured with the electrochemical
585 concentration cell ozonesonde, *Atmos. Meas. Tech.*, 11, 3661-3687,
586 <https://doi.org/10.5194/amt-11-3661-2018>.
- 587 Tarasick, D. W., et al. (2018), Tropospheric Ozone Assessment Report: Tropospheric ozone
588 observations – How well do we know tropospheric ozone changes? *Elementa-Sci.*
589 *Anthropocene*, submitted, 2018.
- 590 Thompson, A. M. (1992), The oxidizing capacity of the Earth's atmosphere: Probable past and
591 future changes. *Science* 256 1157-1165 [doi: 10.1126/science.256.5060.1157]
- 592 Thompson, A. M., K. E. Pickering, D. P. McNamara, M. R. Schoeberl, R. D. Hudson, J. H. Kim,
593 E. V. Browell, V. W. J. H. Kirchhoff and D. Nganga (1996) Where did tropospheric ozone

- 594 over southern Africa and the tropical Atlantic come from in October 1992? Insights from
595 TOMS, GTE/TRACE-A and SAFARI-92, *J. Geophys. Res.*, **101**, 24,251-24,278.
- 596 Thompson, A. M., et al. (2003a), Southern Hemisphere Additional Ozonesondes (SHADOZ)
597 1998–2000 tropical ozone climatology 1. Comparison with Total Ozone Mapping
598 Spectrometer (TOMS) and ground-based measurements, *J. Geophys. Res.*, 108, 8238,
599 doi:10.1029/2001JD000967.
- 600 Thompson, A. M., et al. (2003b), Southern Hemisphere Additional Ozonesondes (SHADOZ)
601 1998–2000 tropical ozone climatology 2. Tropospheric variability and the zonal wave-one, *J.*
602 *Geophys. Res.*, 108, 8241, doi:10.1029/2002JD002241.
- 603 Thompson, A. M., J. C. Witte, S. J. Oltmans and F. J. Schmidlin (2004), SHADOZ (Southern
604 Hemisphere ADDitional Ozonesondes): A tropical ozonesonde-radiosonde network for the
605 atmospheric community, *Bull. Amer. Meteorol. Soc.*, **85**, 1549-1564,
- 606 Thompson, A. M., J. C. Witte, H. G. J. Smit, S. J. Oltmans, B. J. Johnson, V. W. J. H. Kirchhoff,
607 and F. J. Schmidlin (2007), Southern Hemisphere Additional Ozonesondes (SHADOZ)
608 1998–2004 tropical ozone climatology: 3. Instrumentation, station-to-station variability, and
609 evaluation with simulated flight profiles, *J. Geophys. Res.*, 112, D03304,
610 doi:[10.1029/2005JD007042](https://doi.org/10.1029/2005JD007042).
- 611 Thompson, A. M., S. J. Oltmans, D. W. Tarasick, P. von der Gathen, H. G. J. Smit, J. C. Witte,
612 (2011), Strategic ozone sounding networks: Review of design and accomplishments, *Atmos.*
613 *Environ.*, 45, 2145-2163, doi:10.1016/j. atmosenv.2010.05.002.
- 614 Thompson, A. M., et al. (2012) Southern Hemisphere Additional Ozonesondes (SHADOZ)
615 tropical ozone climatology: Tropospheric and tropical tropopause layer (TTL) profiles with

- 616 comparisons to OMI based ozone products. *J. Geophys. Res.*, 117, D23301, doi:
617 10.1029/2010JD016911.
- 618 Thompson, A. M., et al. (2017) First reprocessing of Southern Hemisphere Additional
619 Ozonesondes (SHADOZ) Ozone Profiles (1998-2016). 2. Comparisons with satellites and
620 ground-based instruments, *J. Geophys. Res.*, 122, doi: 10.1002/2017 JD027406.
- 621 Witte, J. C., et al. (2017) First reprocessing of Southern Hemisphere ADditional OZonesondes
622 (SHADOZ) profile records (1998-2015) 1: Methodology and evaluation, *J. Geophys. Res.*,
623 122, doi: 10.1002/2016JD026403.
- 624 Witte, J. C., A. M. Thompson, H. G. J. Smit, H. Vömel, F. Posny and R. Stübi (2018) First
625 reprocessing of Southern Hemisphere Additional Ozonesondes (SHADOZ) Profile Records.
626 3. Uncertainty in ozone profile and total column, *J. Geophys. Res.*, 123, doi: 10.1002/
627 2017JD027791.
- 628 WMO/UNEP, Scientific Assessment of Ozone Depletion: 1990, Global Ozone Research and
629 Monitoring Project - Report No. 25, World Meteorological Organization, Geneva, 1991.
- 630 WMO/UNEP, Scientific Assessment of Ozone Depletion: 1994, Global Ozone Research and
631 Monitoring Project - Report No. 37, World Meteorological Organization, Geneva, 1995.
- 632 WMO/UNEP, Scientific Assessment of Ozone Depletion: 2010, Global Ozone Research and
633 Monitoring Project - Report No. 52, World Meteorological Organization, Geneva, 2011.
- 634 WMO/UNEP, Scientific Assessment of Ozone Depletion: 2014, Global Ozone Research and
635 Monitoring Project - Report No. 55, World Meteorological Organization, Geneva, 2015.

636

637 ***Sidebar 1: Ozone in the Earth's Atmosphere***

638 The ozone molecule (O_3) plays several important roles in the earth's atmosphere. Its
639 absorption of radiation warms the stratosphere, leading to the temperature inversion between
640 troposphere and stratosphere (**Fig. SB1**). The inversion is typically referred to as the tropopause
641 but we use the term "tropopause transition layer" to signify that the tropopause is a region (~130-
642 70 hPa) in which a number of physical properties gradually change. Eighty-ninety percent of the
643 ozone molecules reside in the stratosphere so harmful uv radiation is blocked from reaching the
644 earth's surface. In the free troposphere, ozone acts as a greenhouse gas and is estimated to be
645 responsible for $\frac{1}{4}$ to $\frac{1}{3}$ of earth's warming over the past 200 years. Tropospheric ozone is also
646 a source of the OH free radical, the primary oxidant in the atmosphere, responsible for reacting
647 with hundreds of species (Thompson, 1992). Ozone at the surface is considered a pollutant,
648 harmful to human and plant health when it exceeds 3 mPa (**Fig. SB1**).

649

650

651 *Sidebar 2: Capacity building during JOSIE-SHADOZ*

652

653

A unique feature of JOSIE-SHADOZ was that the ozonesondes were prepared by
654 operators from organizations representing eight SHADOZ sites (see **Fig. 2** showing group
655 photos taken during both sessions in front of the WCCOS chamber). Capacity-building
656 activities during both sessions included lectures on sonde quality-assurance, the importance
657 of metadata reporting, troubleshooting, and training with coaches from sponsoring
658 organizations: NASA/GSFC; NOAA/GMD; KNMI (Netherlands); KMI (Belgium);
659 Meteoswiss, Environment – Climate Change Canada; the Finnish Meteorological Institute.
660 Financial support for the tropical operators came from the UNEP-sponsored Vienna
661 Convention Trust Fund, administered by WMO. Operators are essential contributors to
662 ozonesonde quality assurance by providing detailed metadata information on each sonde
663 launch and maintaining uniformity in their preparation and launch procedures. Bringing

664 together SHADOZ operators for training and knowledge sharing helps to ensure that best
665 practices are applied to operations in a consistent manner across the SHADOZ network.

666

667 *Sidebar 3: Design of the ESC, Reference Instrument, Data System.*

668 The WCCOS, the only one of its kind, was established in the mid-1990s at FZ-Jülich to
669 test, calibrate and compare different types of balloon borne ozonesondes that are used to measure
670 the distribution of ozone in the troposphere and lower/middle stratosphere. The facility is
671 described in more detail in Smit et al. (2000): [http://www.fz-juelich.de/iek/iek-](http://www.fz-juelich.de/iek/iek-8/EN/Expertise/Infrastructure/ESF/ESF_node.html)
672 [8/EN/Expertise/Infrastructure/ESF/ESF_node.html](http://www.fz-juelich.de/iek/iek-8/EN/Expertise/Infrastructure/ESF/ESF_node.html).

673 The setup of the simulation facility (Fig. **SB2a**), consists of four major components:

- 674 1. Environmental Simulation Chamber. The ESC chamber is a temperature-controlled vacuum
675 chamber with a test room volume of about 500 liter (80 x 80 x 80 cm). Within the ESC the
676 pressure and temperature can be dynamically regulated, with pressures between 5 and 1000
677 hPa and temperatures between 200 and 300 K, with a maximum rate of $\pm 2\text{K}/\text{min}$. Iso-
678 thermically operated, the temperature variations of the air as well as the wall inside the test
679 room can be maintained within $\pm 0.2\text{ K}$. For more details see Smit et al. (2000).
- 680 2. Ozone Photometer (OPM), Ozone reference. The OPM is a fast response dual-beam UV-
681 absorption photometer, originally developed by Proffitt and McLaughlin (1983) for use on
682 stratospheric balloons. The instrument was flown during Balloon Ozone Intercomparison
683 (BOIC) missions in 1983/1984 (Hilsenrath et al., 1986); it was used in the Balloon
684 Experiment on Standards for Ozone Sondes (BESOS) field campaign in Wyoming, in 2004
685 (Deshler et al., 2008). The OPM is an absolute measuring device with a 1-s response time at
686 a sampling volume flow rate of about 8 l/min. The overall accuracy of ozone measurements

687 made by the OPM is better than $\pm 2\%$ for simulated altitudes up to 25 km (pressures down to
688 25 hPa) and $\pm 3.5\%$ at 30-35 km altitude (12-5 hPa). The instrument resides in a separate
689 vacuum vessel which is connected to the ESC such that the UV-photometer has the same
690 pressure conditions as inside the test chamber.

691 3. Ozone profile simulator (OPS). A gas-flow system that controls the ozone concentrations
692 sampled by the instruments in the ESC, with a gas flow rate of 12-15 l/min. The OPS can
693 simulate vertical ozone profiles between the surface and 35 km. The OPS can accommodate
694 up to four ozonesondes, including the OPM (Fig. **SB2b**). The OPS has an option to specify
695 ozone step functions or zero ozone to investigate the response time and background
696 characteristics of ozonesondes.

697 4. Data Acquisition System (DAS). The entire simulation process is automated by computer
698 control in order to have reproducible conditions with respect to the simulated pressure,
699 temperature and ozone versus time, and for recording and storing the large variety of
700 parameters measured during the simulation process. A special electronic interface (JOSIE/
701 ECC-interface) couples the ECC sonde to the DAS, transmitting cathode cell current, pump
702 temperature, pump motor current and pump motor voltage (12V). A small variable electrical
703 heater (0-10W) adjusts pump temperatures to values similar to actual flight temperatures.

1 **Table List:**2 **Table 1: JOSIE activities on ozonesonde procedures and related reports.**

Campaign	Objective
JOSIE-1996 GAW Report #130	<ul style="list-style-type: none"> • Operating Procedures • Profiling Capabilities • Intercomparison sonde types (ECC, Brewer Mast, Meisei)
JOSIE-1998 GAW Report #57	<ul style="list-style-type: none"> • Manufacturing ECC sondes (SPC, ENSCI)
JOSIE-2000 GAW Report #158 (Smit et al., 2007)	<ul style="list-style-type: none"> • Operating Procedures • Focus on ECC sonde <ul style="list-style-type: none"> ○ Different sensing solution types ○ Different manufacturers (SPC, ENSCI)
BESOS-2004 (Deshler et al., 2008)	<ul style="list-style-type: none"> • Operating Procedures under flight conditions • Focus on ECC sonde <ul style="list-style-type: none"> ○ Different sensing solution types ○ Different manufacturers (SPC, ENSCI)
ASOPOS 2002-2012 GAW Report #201	<ul style="list-style-type: none"> • Define and establish Standard Operating Procedures for ECC sondes
JOSIE-2009	<ul style="list-style-type: none"> • Manufacturers (SPC, ENSCI)
JOSIE-2010	<ul style="list-style-type: none"> • Refurbished sondes
O3S-DQA Guidelines Report-2012	<ul style="list-style-type: none"> • Homogenization and Uncertainties
JOSIE-SHADOZ-2017	<ul style="list-style-type: none"> • Operating procedures • Tropical simulations • Different sensing solution types • Different manufacturers (SPC, ENSCI)

3

4 **Table 2: SHADOZ stations operating at least 10 years between 1998 and 2017**

Station	Latitude, Longitude	Current ECC Sensor	Current Radiosonde
Pago Pago, Am. Samoa	14.23S, 170.56W	ENSCI	iMet-1
Hilo, Hawaii	19.40N, 155.00W	ENSCI	iMet-1
San Cristobal, Galapagos, Ecuador	0.92S, 89.60W	ENSCI	Vaisala RS92
San Pedro, Costa Rica	9.94N, 84.04W	ENSCI	iMet-1
Paramaribo, Surinam	5.81N, 55.21W	SPC	Vaisala RS92
Ascension Is., U.K	7.98S, 14.42W	ENSCI	iMet-1
Natal, Brazil	5.42S, 35.38W	SPC	Lockheed-Martin-Sippican LMS6
Irene, S. Africa	25.90S, 28.22E	SPC	Vaisala RS92
Nairobi, Kenya	1.27S, 36.80E	ENSCI	Vaisala RS92
La Réunion, France	21.10S, 55.48E	ENSCI	Modem M10
Kuala Lumpur, Malaysia	2.73N, 101.70E	ENSCI	GRAW DFM-09
Hanoi, Vietnam	21.02N, 105.80E	ENSCI	Vaisala RS92
Watukosek-Java, Indonesia	7.57S, 112.65E	ENSCI	---*
Suva, Fiji	18.10S, 178.40E	ENSCI	iMet-1

5 *Operated Meisei RS II-KC79D radiosonde-ozonesonde system 1992-1999; Vaisala RS80 1998-2013.

6

7 **Table 3: SHADOZ station operators and instruments tested in JOSIE. Stations 1-4**
 8 **participated in Session 1 (9-20 October 2017); stations 5-8 participated in Session 2 (23**
 9 **October – 3 November 2017).**

Participant Number	SST	Operator	Affiliation	Station
Session 1				
1	1.0% Full Buffer	Tshidi Machinini	South African Weather Service	Irene, South Africa
2	1.0% Full Buffer	Francisco R. da Silva	Brazilian Space Agency	Natal, Brazil
3	0.5% Half Buffer	Kennedy Thiong'o	Kenyan Meteorological Department	Nairobi, Kenya
4	0.5% Half Buffer	Ernesto Corrales	University of Costa Rica	San Pedro, Costa Rica
Session 2				
5	1.0% Full Buffer	George Paiman	Meteorological Service of Suriname	Paramaribo, Surinam
6	0.5% Half Buffer	Zamuna Zainal	Malaysian Meteorological Department	Kuala Lumpur, Malaysia
7	0.5% Half Buffer	Françoise Posny	Université La Réunion, Météo-France, CNRS	La Réunion Is., France
8	0.5% Half Buffer	Nguyen Thi Hoang Anh	Vietnam Meteorological and Hydrological Administration	Hanoi, Vietnam

10

11 **Table 4: Characteristics of JOSIE-SHADOZ-2017 simulations in the WCCOS chamber**
 12 **with Simulation Numbers listed for the two Sessions. LT=lower troposphere, MT=mid-**
 13 **troposphere, UT=upper troposphere and LS=lower-stratosphere. All profiles simulated**
 14 **with nominal 5 m/s ascent velocity. The tropopause was located at Z=18-20 km with**
 15 **minimum temperature ~-(70-80)°C. The stratospheric profile was specified to be the same**
 16 **for all simulations.**

Session 1				
Simulation Number	Troposphere Profile Type	Profile Type Index**	Specifications	ECC Procedure
171	Recent deep convection	1	Extremely low O ₃ values nearly uniformly up to tropopause with very steep gradient into LS	Station-supplied SST & procedures
172	Maritime background	2	Low O ₃ in LT, moderate O ₃ in MT, extremely low O ₃ in UT	Station-supplied SST & procedures

173, 174, 175, 176*	Biomass burning	3	Enhanced O ₃ in LT, high O ₃ in MT, low O ₃ in UT	Station-supplied SST & procedures
177, 178, 179, 181	Biomass burning	3	Enhanced O ₃ in LT, high O ₃ in MT, low O ₃ in UT	JOSIE-supplied SST & WMO procedures
180	Maritime background	2	Low O ₃ in LT, moderate O ₃ in MT, extremely low O ₃ in UT	JOSIE-supplied SST & WMO procedures
Session 2				
Simulation Number	Troposphere Profile Type	Profile Type Index**	Specifications	ECC Procedure
182, 183, 184,186	Biomass burning	3	Enhanced O ₃ in LT, high O ₃ in MT, low O ₃ in UT	Station-supplied SST & procedures
185	Maritime background	2	Low O ₃ in LT, moderate O ₃ in MT, extremely low O ₃ in UT	Station-supplied SST & procedures
187, 188, 190, 191	Biomass burning	3	Enhanced O ₃ in LT, high O ₃ in MT, low O ₃ in UT	JOSIE-supplied SST & WMO procedures
189	Maritime background	2	Low ozone in LT, enhanced ozone in MT and extreme low ozone in UT	JOSIE-supplied SST & WMO procedures

17 * Due to a problem with the ESC, Simulation 176 only recorded profiles to 15 km.

18 ** In Figure 4, 1 = blue, 2= green, 3= red

19

20 **Table 5: Total and partial column statistics from two SHADOZ simulations and means for**

21 **all 10 simulations (five each in Sessions 1 and 2). All simulations use SHADOZ SOPs.**

Instrument	Sim 171 (DU)	Sim 182 (DU)	Mean OPM/Sonde Ratio: TCO	Mean OPM/Sonde Ratio: Trop O ₃ (0-15 km)	Mean OPM/Sonde Ratio: TTL O ₃ (12-18 km)	Mean OPM/Sonde Ratio: Strat O ₃ (15 km-end)
OPM	282	-----	337 DU	47.0 DU	4.93 DU	298 DU
Participant 1	1.07	-----	1.03	1.09	1.02	1.04
Participant 2	1.09	-----	1.04	1.09	1.03	1.04
Participant 3	1.03	-----	1.03	1.02	0.95	1.03
Participant 4	1.01	-----	1.02	1.06	1.01	1.02
OPM	-----	334	313 DU	41.0 DU	5.30 DU	271 DU
Participant 5	-----	1.00	1.03	0.85	0.77	1.03
Participant 6	-----	1.04	1.04	0.89	0.87	1.05
Participant 7	-----	1.07	1.04	0.93	0.93	1.05
Participant 8	-----	1.00	1.02	0.88	0.87	1.02

22

23 **Table 6: Total and partial column statistics from profile simulations, relative to OPM,**

24 **categorized by SOP and sonde/solution types.**

Methodology	No.	Mean Sonde/OPM TCO	Mean Sonde/OPM Trop O ₃ (0-15 km)	Mean Sonde/OPM TTL O ₃ (12-18 km)	Mean Sonde/OPM Strat O ₃ (20 km-end)
SHADOZ SOP	40	1.03	1.01	0.94	1.04
JOSIE SOP	40	0.97	0.99	0.94	0.97
ENSCI 1.0%, 0.1B*	25	0.98	1.00	0.97	0.98
SPC 1.0%, 0.1B	10	0.97	0.96	0.90	0.98
ENSCI 0.5%, 0.5B	20	1.03	1.00	0.91	1.04
SPC 1.0%, 1.0B	15	1.03	1.01	0.95	1.04
ENSCI 2.0%, 0.1B	5	0.97	1.01	0.97	0.97
SPC 2.0%, 0.1B	5	0.97	0.94	0.90	0.96

25 * B=Buffer

26 *Figure Caption List:*

27

28 **Figure 1: Map of SHADOZ stations.**

29

30 **Figure 2(a): Session 1 participants: (1) George Brothers (NASA/WFF); (2) Kennedy**
31 **Thiong'o (Kenya Met Dept.); (3) Francisco Raimundo da Silva (INPE Natal); (4) Ernesto**
32 **Corrales (Univ. Costa Rica); (5) Peter von der Gathen (Alfred Wegener Institute); (6)**
33 **Herman Smit (FZ Jülich); (7) Ryan Stauffer (NASA/GSFC); (8) Gary Morris (St.**
34 **Edward's Univ.); (9) Gabi Nork (FZ Jülich); (10) Anne Thompson (NASA/GSFC); (11)**
35 **Bryan Johnson (NOAA ESRL); (12) Tshidi Machinini (South African Weather Service);**
36 **(13) Tatsumi Nakano (Japan Met Agency); (14) Rhonie Wolff (NASA/WFF).**

37

38 **Figure 2(b): Session 2 participants: (1) Gonzague Romanens (MeteoSwiss); (2) Torben**
39 **Blomel (FZ Jülich); (3) Jennifer Gläser (FZ Jülich); (4) Nguyen Thi Hoang Anh (Vietnam**
40 **Meteorological and Hydrological Administration); (5) Anne Thompson (NASA/GSFC); (6)**
41 **Jonathan Davies (Env. Climate Change Canada); (7) Zamuna Zainal (Met Malaysia); (8)**
42 **Patrick Neis (FZ Jülich); (9) Gabi Nork (FZ Jülich); (10) Rigel Kivi (FMI); (11) Rene Stübi**
43 **(MeteoSwiss); (12) Patrick Cullis (NOAA ESRL); (13) Herman Smit (FZ Jülich); (14) Marc**
44 **Allaart (KNMI); (15) Roeland Van Malderen (Royal Meteorological Institute of Belgium);**
45 **(16) Jacquelyn Witte (NASA/GSFC); (17) George Paiman (Met Dept. of Suriname); (18)**
46 **Andreas Petzold (FZ Jülich); (19) Gilbert Levrat (MeteoSwiss); (20) Françoise Posny**
47 **(Univ. of La Réunion).**

48

49 **Figure 3: (a) Schematic of an electrochemical concentration cell (ECC) in operational**
50 **mode. (b) ECC instrument in Styrofoam box in which it is housed during JOSIE tests or in**
51 **deployment (when launched the sensor is sealed with a Styrofoam lid). Instrument and**
52 **solution type for each JOSIE-SHADOZ station appear in Tables 2 and 3, respectively.**

53

54 **Figure 4: Simulated ozone profiles (in partial pressure) as a function of simulation time for**
55 **the troposphere and stratosphere until 33 km altitude (a) and up to 20 km in (b). Three**
56 **different tropospheric ozone profiles with extreme low ozone concentrations up to the**
57 **tropopause (Altitude \approx 18 km) in blue and two profiles with moderate to enhanced middle**
58 **tropospheric ozone values in green and red, respectively.**

59

60 **Figure 5: Ozone “raw” profiles of typical simulations in Sessions 1 (a) and 2 (b).**
61 **Participants are listed in Table 3, simulation specifications are listed in Table 4.**

62

63 **Figure 6: (a) Participant mean profiles relative to OPM in partial pressure (mPa), and (b)**
64 **% deviation ($\text{Sonde} - \text{OPM} / \text{OPM}$). Based on 5 simulations per participant.**

65

66 **Figure 7: Same as Fig. 6, except for JOSIE SOP as described in Table 4.**

67

68 **Figure 8: (a) Session 1 SHADOZ SOP (blue) and JOSIE SOP (red) mean profiles**
69 **subtracted from the OPM profile mean; (b) Session 2 JOSIE 2.0.1 (black) and JOSIE 1.0.1**
70 **(red) SST profile means subtracted from the OPM; and (c) Session 1 and 2 mean profiles of**

71 **ENSCI-OPM (red) and SPC-OPM (blue) for which JOSIE 1.0.1 SST and SOP was used. 1-**
72 **sigma standard deviations for all panels are included.**

73

74 **Figure SB1. Ozone and temperature profiles from a typical SHADOZ sounding at Natal,**
75 **Brazil, taken from the archive, <https://tropo.gsfc.nasa.gov/shadoz>.**

76

77 **Figure SB2: (a) Set up for the simulation of vertical ozone soundings with a schematic of**
78 **the Environmental Simulation Chamber, showing Ozone Photometer (OPM) standard**
79 **reference, control systems, placement of four ozonesondes (“TEO”) in the chamber and**
80 **data acquisition system (DAS). (b) Photo of the chamber and DAS computer.**

81



Fig. 1. Map of SHADOZ stations.

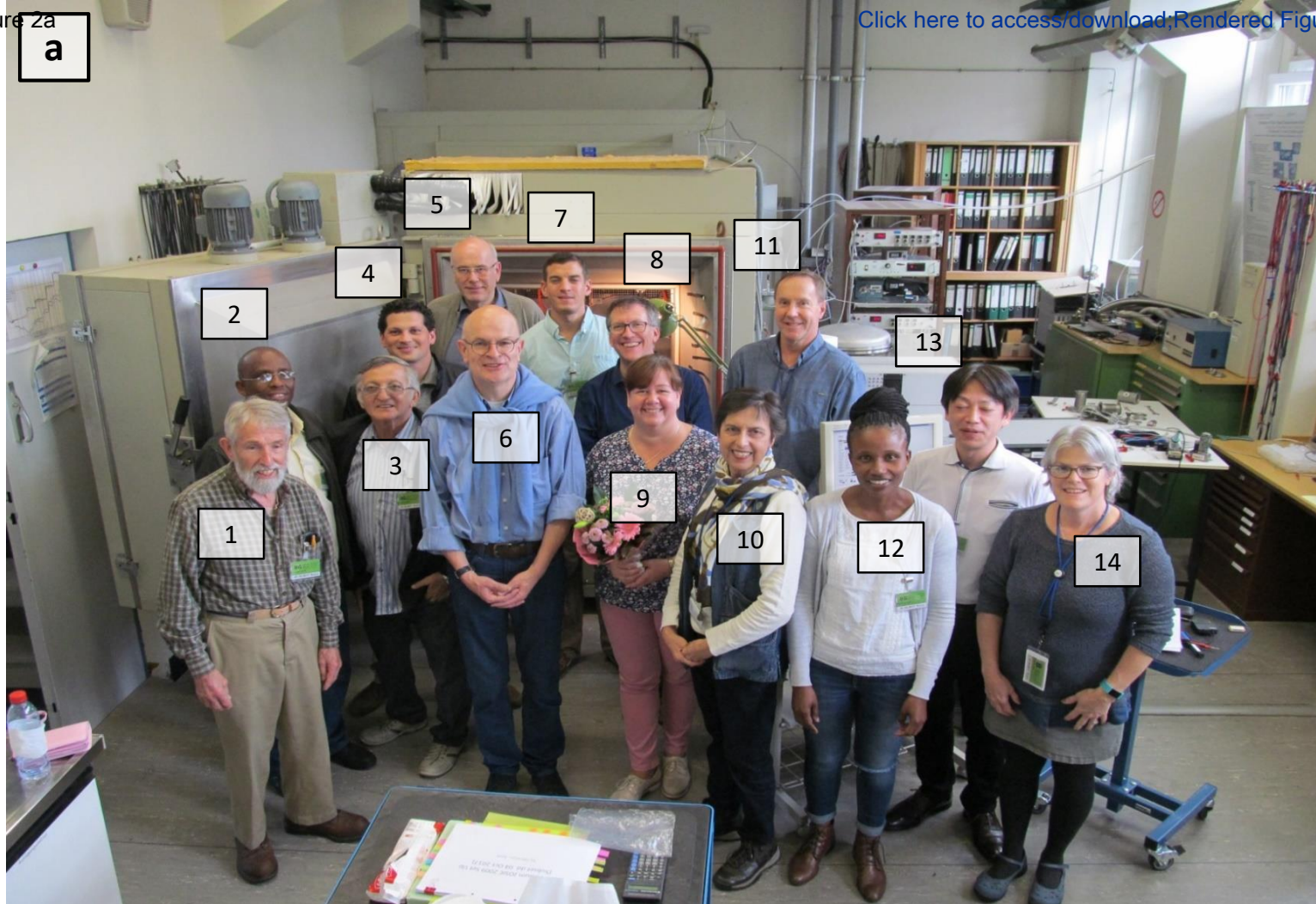


Fig. 2. (a) Session 1 participants: (1) George Brothers (NASA/WFF); (2) Kennedy Thiong'o (Kenya Met Dept.); (3) Francisco Raimundo da Silva (INPE Natal); (4) Ernesto Corrales (Univ. Costa Rica); (5) Peter von der Gathen (Alfred Wegener Institute); (6) Herman Smit (FZ Jülich); (7) Ryan Stauffer (NASA/GSFC); (8) Gary Morris (St. Edward's Univ.); (9) Gabi Nork (FZ Jülich); (10) Anne Thompson (NASA/GSFC); (11) Bryan Johnson (NOAA ESRL); (12) Tshidi Machinini (South African Weather Service); (13) Tatsumi Nakano (Japan Met Agency); (14) Rhonie Wolff (NASA/WFF).



Fig. 2. (b) Session 2 participants: (1) Gonzague Romanens (MeteoSwiss); (2) Torben Blomel (FZ Jülich); (3) Jennifer Gläser (FZ Jülich); (4) Nguyen Thi Hoang Ahn (National Hydro-Meteorological Service of Vietnam); (5) Anne Thompson (NASA/GSFC); (6) Jonathan Davies (Env. Climate Change Canada); (7) Zamuna Zainal (Met Malaysia); (8) Patrick Neis (FZ Jülich); (9) Gabi Nork (FZ Jülich); (10) Rigel Kivi (FMI); (11) Rene Stübi (MeteoSwiss); (12) Patrick Cullis (NOAA ESRL); (13) Herman Smit (FZ Jülich); (14) Marc Allaart (KNMI); (15) Roeland Van Malderen (Royal Meteorological Institute of Belgium); (16) Jacquelyn Witte (NASA/GSFC); (17) George Paiman (Met Dept. of Suriname); (18) Andreas Petzold (FZ Jülich); (19) Gilbert Levrat (MeteoSwiss); (20) Françoise Posny (Univ. of La Réunion).

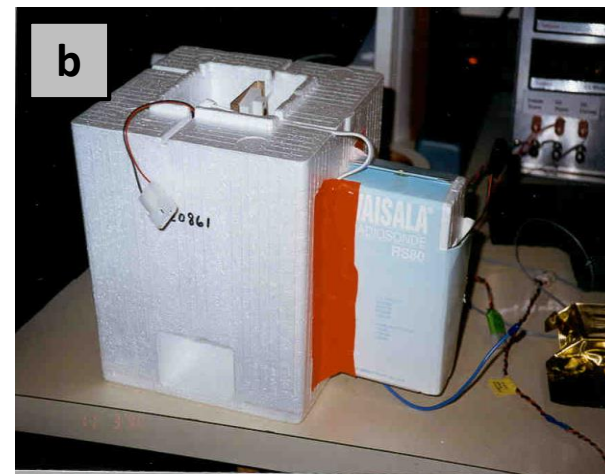
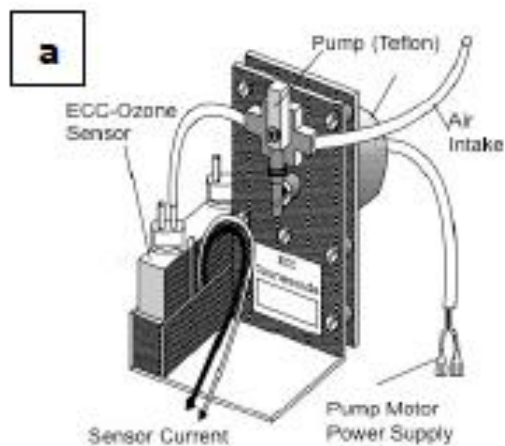


Figure 3: (a) Schematic of an electrochemical concentration cell (ECC) in operational mode. (b) ECC instrument in Styrofoam box in which it is housed during JOSIE tests or in deployment (when launched the sensor is sealed with a Styrofoam lid). Instrument and solution type for each JOSIE-SHADOZ station appear in Tables 2 and 3, respectively.

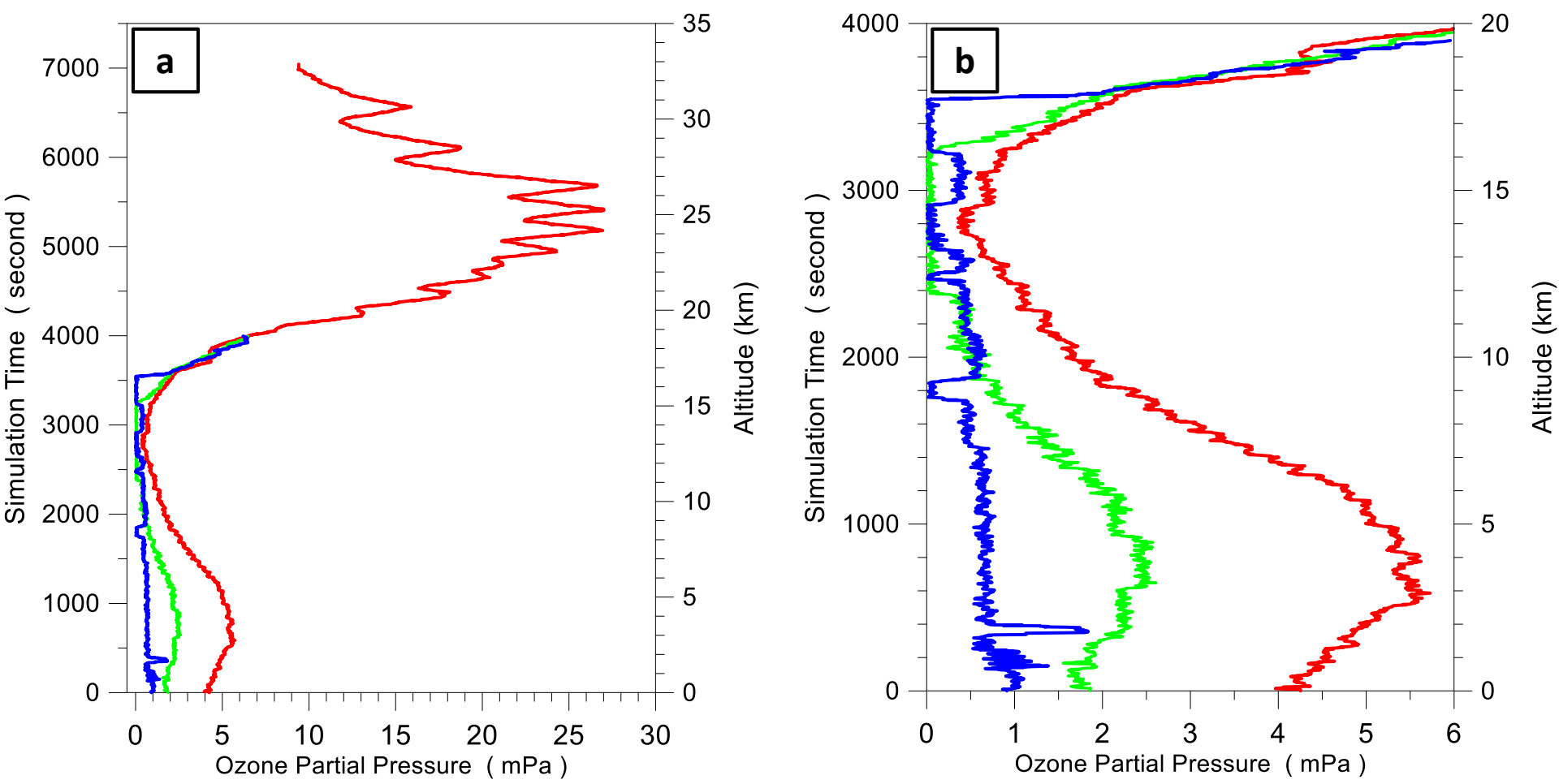


Fig. 4. Simulated ozone profiles (in partial pressure) as a function of simulation time for the troposphere and stratosphere until 33 km altitude (a) and up to 20 km in (b). Three different tropospheric ozone profiles with extreme low ozone concentrations up to the tropopause (Altitude \approx 18 km) in blue and two profiles with moderate to enhanced middle tropospheric ozone values in green and red, respectively.

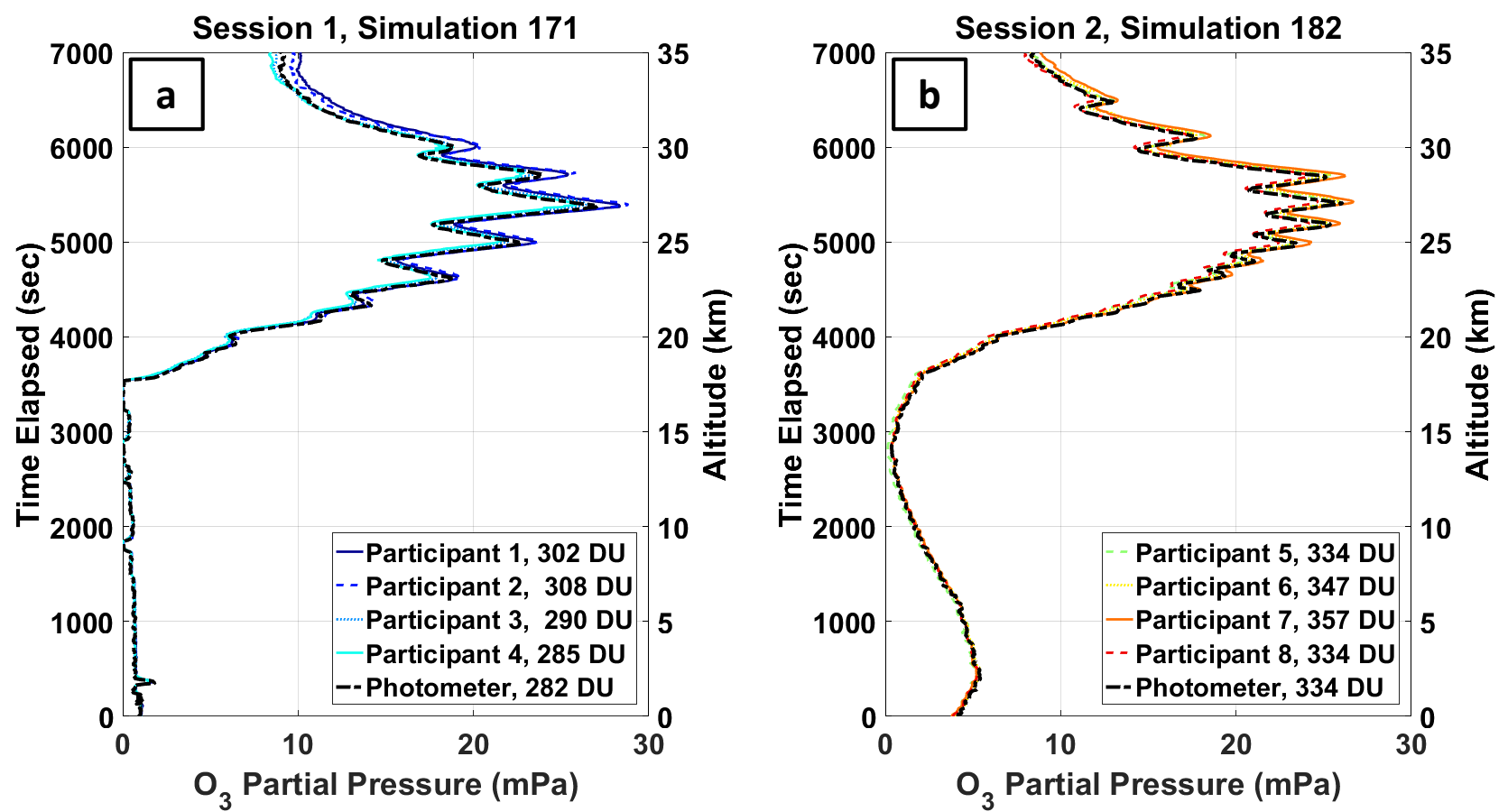


Fig. 5. Ozone “raw” profiles of typical simulations in Sessions 1 (a) and 2 (b). Participants are listed in Table 3, simulation specifications are listed in Table 4.

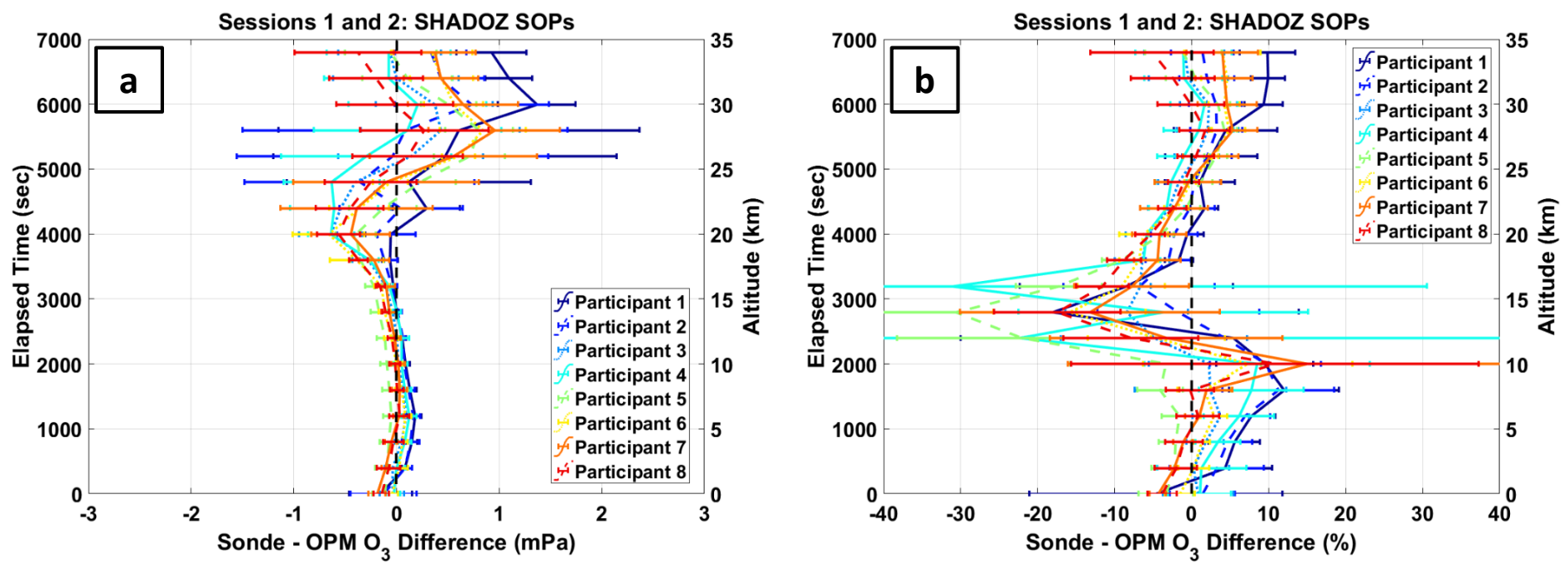


Fig. 6. (a) Participant mean profiles relative to OPM in partial pressure (mPa), and (b) % deviation (Sonde – OPM / OPM). Based on 5 simulations per participant.

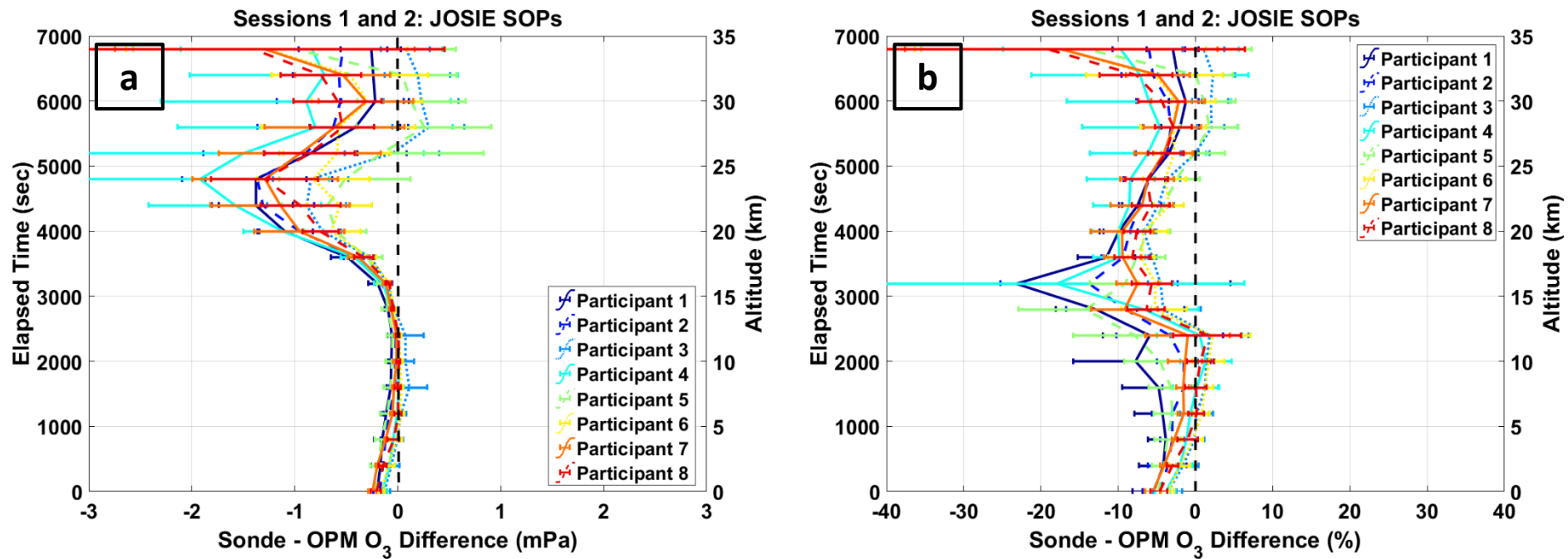


Fig. 7. Same as Fig. 6, except for JOSIE SOP as described in Table 4.

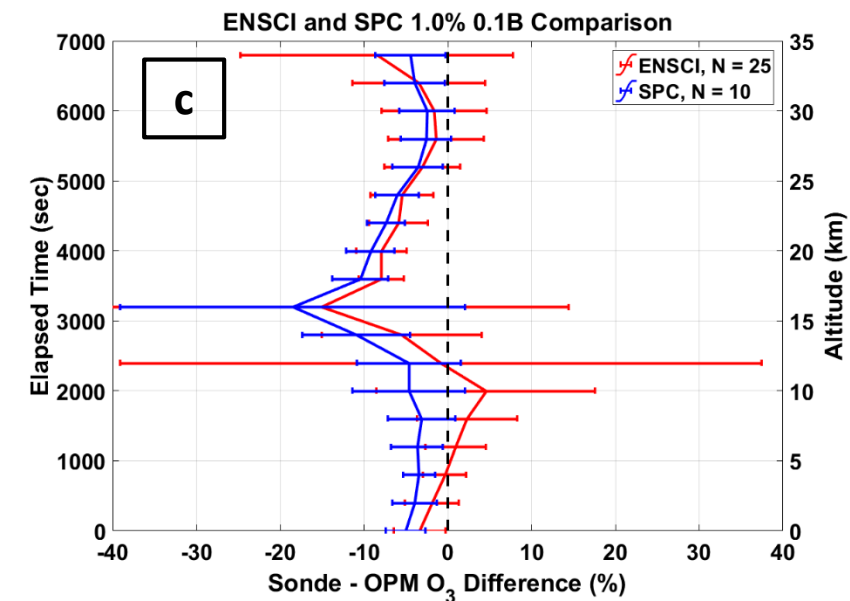
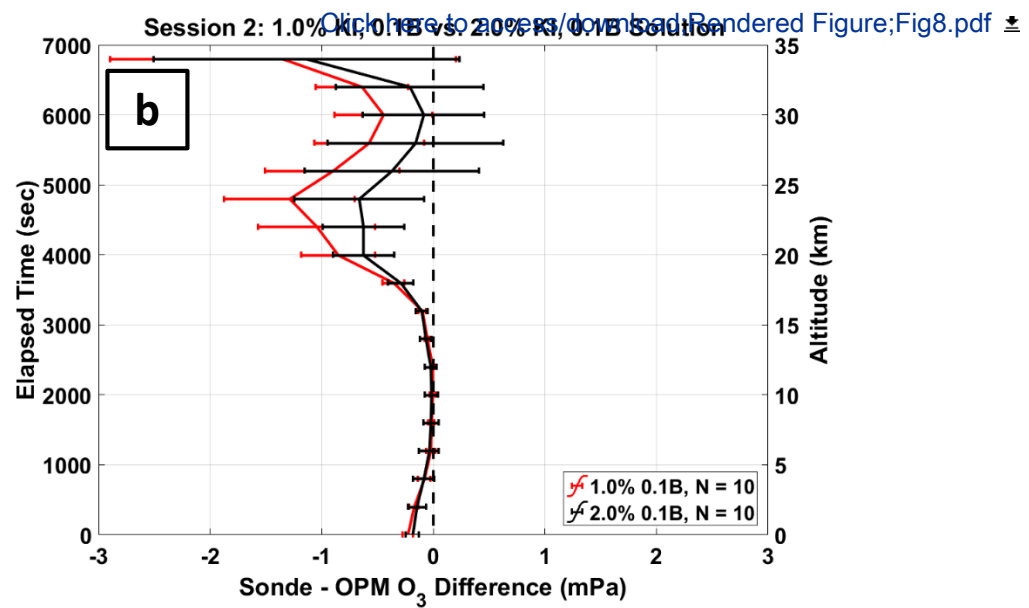
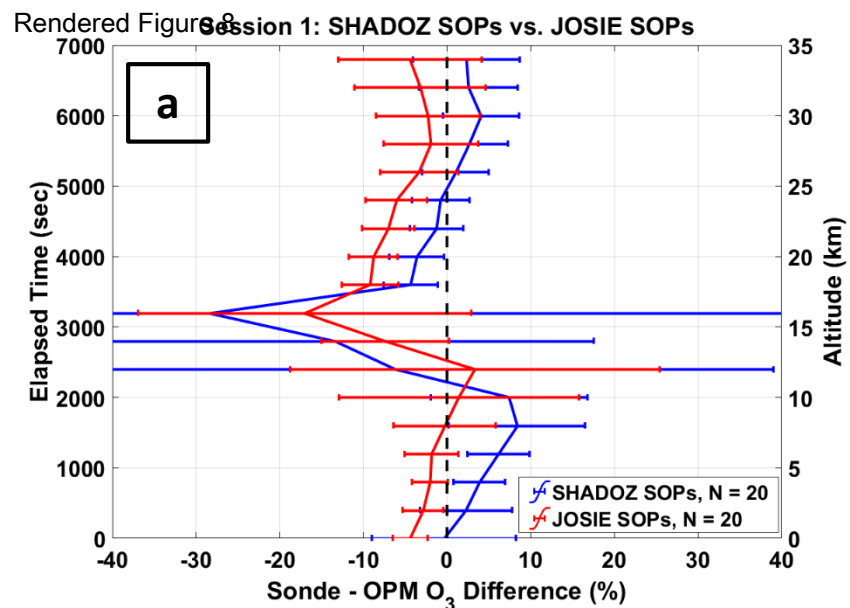
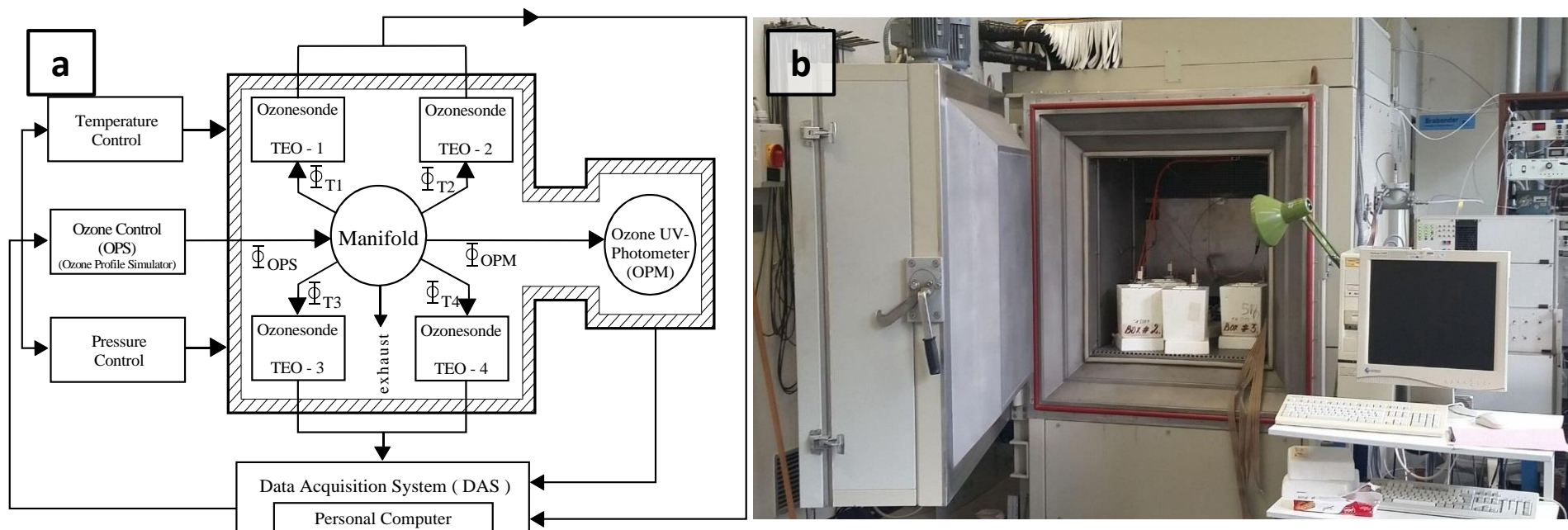


Fig. 8. (a) Session 1 SHADOZ SOP (blue) and JOSIE SOP (red) mean profiles subtracted from the OPM profile mean; (b) Session 2 JOSIE 2.0.1 (black) and JOSIE 1.0.1 (red) SST profile means subtracted from the OPM; and (c) Session 1 and 2 mean profiles of ENSCI-OPM (red) and SPC-OPM (blue) for which JOSIE 1.0.1 SST and SOP was used. 1-sigma standard deviations for all panels are included.



SB2. (a) Set up for the simulation of vertical ozone soundings with a schematic of the Environmental Simulation Chamber, showing Ozone Photometer (OPM) standard reference, control systems, placement of four ozonesondes in the chamber (“TEO”) and data acquisition system (DAS). (b) Photo of the chamber and DAS computer.